涡轮增压柴油机和火花点火式发动机

TURBOCHARCED DIESEL AND SPARK IGNITION ENGINES

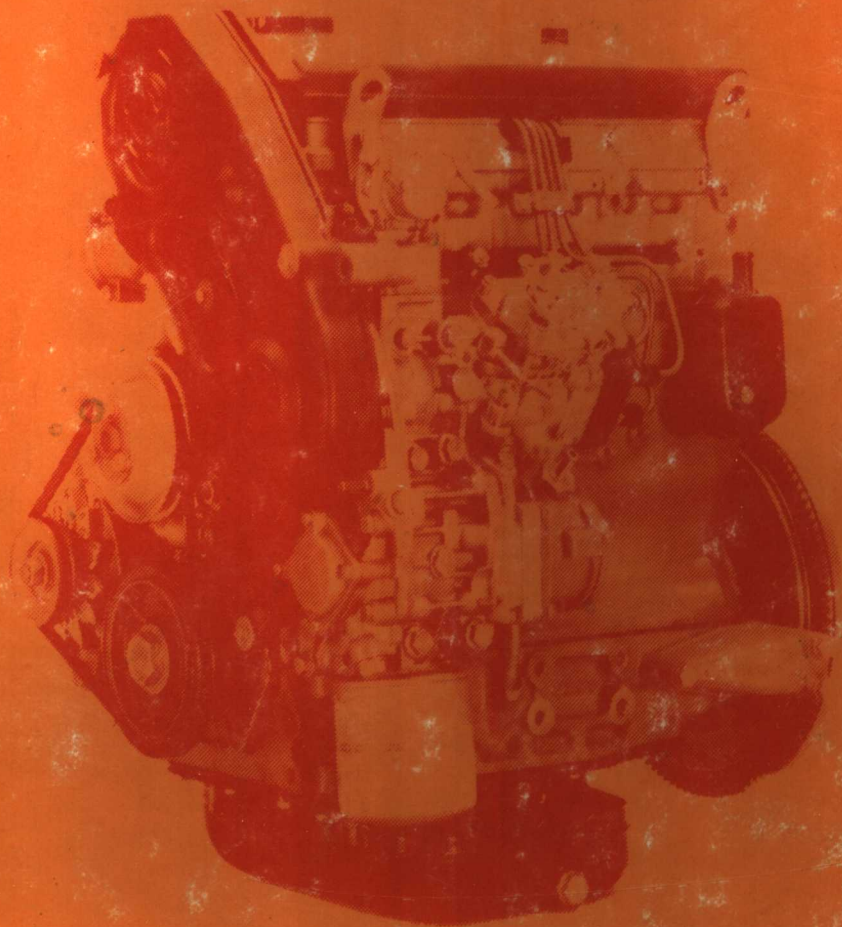

SAE The Engineering Resource For Advancing Mobility

PROGRESS IN TECHNOLOGY SERIES
NO. 23

TURBOCHARGED DIESEL AND SPARK IGNITION ENGINES

(Selected papers through 1981)

Prepared under the auspices
of the Powerplant Activity

Published by:
SAE
400 Commonwealth Dr.
Warrendale, PA 15096

ISBN 0-89883-111-3
SAE/PT-81/23

Library of Congress Catalog Card Number: 81-52645
Printed in U.S.A.

Manufactured by Publishers Choice Book Mfg. Co.
Mars, Pennsylvania 16046

PREFACE

TURBOCHARGERS EXPERIENCED enormous growth and acceptance on the diesel engine during the 1970's. With today's emphasis on increased fuel economy, there are many who predict that the 1980's will be a decade of increased usage of the turbocharger on spark ignition engines, especially as these engines become smaller. This book contains an assemblage of papers that were chosen individually and as a group to be useful to engineers interested in becoming knowledgable on all types of turbocharged engines.

The editors have reviewed all SAE papers dealing with turbocharging. The papers were classified and reviewed not only to select the most outstanding papers, but also on the basis of selecting an assemblage of papers which provides as broad a coverage as is possible of the most important aspects of turbocharging. This review included preparation of a matrix of 22 topics which are covered by the papers included in the book. This matrix is included on the following page and reviewing it will allow the reader to select those papers which cover the subject matter on turbocharging of interest to him/her. It will be noted that the more important topics are covered by several papers. Another of the editors' goals was to insure that all topics are covered by at least one of the included papers. More papers on turbochargers are listed in the bibliography.

In reviewing the topics covered by all the SAE papers on turbochargers, it is obvious that several important topics have not been addressed or warrant additional technical literature. As a result, turbocharger engineers are encouraged to prepare SAE papers on these subjects. Some examples of topics where new technical papers will complement existing literature would be compressor and turbine design, transient response of turbochargers, blade vibration, and fatigue induced by turbocharger speed variations during operation.

In addition, an effort was made to include quality papers which present an introduction to several air charging systems which have been developed, or are being developed, for the purpose of complementing or replacing the turbocharger.

The editors hope that you will find this book to be a reference source of introductory information on all aspects of turbochargers and turbocharged engines.

Max E. Rumbaugh, Jr., Chairman
Charles J. Raffa
Mel R. L'Ecuyer
Editorial Advisory Committee

TURBOCHARGING DIESEL AND SPARK IGNITION ENGINES
MATRIX OF TOPICS COVERED IN PAPERS

Paper #	Adiabatic Engines	After Cooling	Aircraft	Altitude (Ground Vehicle)	Automobile	Ceramics	Compound Bottoming	Comprex	Computer Simulations	Diesel Engines	Emissions	Gasoline Engines	Hyperbar	Manifolding	Matching Turbos	Series Turbocharging	Supercharging	Transient Response	Turbine Assisted	Turbine Compressors	Two Stroke	Variable Geometry
800289						X			X		X	X										
790312												X										
780413												X			X			X				
790762					X					X												
720783										X												
810003					X			X		X		X	X	X			X				X	
740740										X					X	X						
810341		X		X				X		X					X	X			X			
790069										X				X				X		X		
770123									X	X					X			X				
790278									X	X					X							
770122									X	X	X							X	X			
750797										X	X											
790316									X	X	X											
710822				X					X	X												
690309		X	X						X			X										
660744				X	X					X												
770756							X			X			X			X						
740723										X			X									
810343					X			X		X							X	X				
780686	X	X					X			X		X										
810523					X	X				X												
810336										X					X							X

EDITORIAL ADVISORY COMMITTEE PREPARING PT-23

Max E. Rumbaugh, Jr., Chairman
Schwitzer, Wallace Murray Corporation

Charles J. Raffa
Tank Automotive Research and Development Command
United States Army

Mel R. L'Ecuyer
Purdue University

TABLE OF CONTENTS

SI, DIESEL AUTO, TWO STROKE

MATCHING, MANIFOLDING, AND TRANSIENT RESPONSE

COMPUTER SIMULATIONS AND EMISSIONS

ALTITUDE AND AMBIENT COMPENSATION

ALTERNATIVE SYSTEMS AND MATERIALS

Simulation Studies of the Effects of Turbocharging and Reduced Heat Transfer on Spark-Ignition Engine Operation**

Paula A. Watts
and John B. Heywood
Sloan Automotive Lab
Massachusetts Institute of Technology
Cambridge, MA

ABSTRACT

A computer simulation of the four-stroke spark-ignition engine cycle has been used to examine the effects of turbocharging and reduced heat transfer on engine performance, efficiency and NO_x emissions. The simulation computes the flows into and out of the engine, calculates the changes in thermodynamic properties and composition of the unburned and burned gas mixtures within the cylinder through the engine cycle due to work, heat and mass transfers, and follows the kinetics of NO formation and decomposition in the burned gas. The combustion process is specified as an input to the program through use of a normalized rate of mass burning profile. From this information, the simulation computes engine power, fuel consumption and NO_x emissions.

Wide-open-trottle predictions made with the simulation were compared with experimental data from a 5.7ℓ naturally-aspirated and a 3.8ℓ turbocharged production engine. The predicted trends of mean effective pressure and fuel consumption showed acceptable agreement with the data.

Simulation studies were performed to compare the fuel consumption and NO_x emissions of a 5.7ℓ naturally aspirated engine with a 3.8ℓ turbocharged engine over the complete load and speed range. These engines have equal maximum power. Further studies were carried out to examine the effects of reduced heat transfer on engine performance, efficiency and NO_x emissions. Reductions in heat transfer were simulated by increasing the thermal boundary layer resistance, and through the use of ceramic materials on selected engine components over a range of combustion chamber wall temperatures.

BACKGROUND

Computer simulations of the complete cycle of the four-stroke spark-ignition engine can be used to examine the effect of changes in operating and design variables on engine performance, efficiency and emissions. The details of several of these simulations which can be used for this purpose have been previously published: e.g. (1), (2).* These types of simulations are "thermodynamic" or "zero-dimensional" in structure; that is, their formulation is based on the first law of thermodynamics and no attempt is made to include the geometric details of the combustion chamber and the shape of the flame front.

The inputs to the calculation are: engine geometry, engine speed, intake mixture fuel-air equivalence ratio, exhaust gas recycle fraction, intake manifold pressure, combustion chamber component wall temperatures, and parameters which define the mixture burning rate. One-dimensional quasi-steady

*Numbers in parentheses designate References at end of paper.

**Paper 800289 presented at the Congress and Exposition, Detroit, Michigan, February 1980.

flow equations are used to obtain the mass flow through the valves during the intake and exhaust processes. The first law of thermodynamics is used to determine the conditions in the engine cylinder during each portion of the four-stroke cycle: intake, compression, expansion and exhaust. Empirical correlations are used for heat transfer between the gas in the cylinder and the walls, in conjunction with a simple boundary layer model.

The cycle simulation then predicts the following: mass flow rate of fuel and air through the engine, the cylinder pressure, unburned and burned mixture temperatures, heat transfer to the combustion chamber walls and work transfer to the piston, all as functions of crank angle during the cycle. From this information, the indicated power, specific fuel consumption, efficiency, mean effective pressure and mean exhaust temperature are then computed for the particular engine operating point under study. Estimates of engine friction are then used to obtain brake valves of these quantities.

The calculated cylinder pressure and burned gas temperature profiles, with the equivalence ratio and fuel composition, can be used in parallel to compute the rate of formation and decomposition of nitric oxide (NO) in the burned gases through the combustion and expansion processes. In this manner, the engine exhaust NO concentration and specific emissions are obtained.

SCOPE OF THIS STUDY

These spark-ignition engine simulations have been validated and used primarily at part-throttle engine operating conditions. These engine conditions are of greatest importance for emissions reductions and fuel economy improvements under typical driving conditions. However, wide-open-throttle performance determines the displacement of an engine for a given application, which in turn influences the fuel economy at part-throttle. In this paper, we evaluate the wide-open-throttle predictions of a previously developed cycle simulation (2) against experimental data from both a naturally-aspirated and a turbocharged production engine. We then use the simulation to compare the fuel consumption and NO_x emissions and characteristics of these two engines over the complete load and speed range. This example illustrates the usefulness of a cycle simulation of this type in first sizing two different engine concepts to provide the same performance characteristics (their wide-open-throttle performance), and then in comparing their operating characteristics at the same brake-load and speed in the part-throttle load regime.

We also use the simulation to examine various aspects of the effect of heat transfer on engine performance, efficiency and NO_x emissions. These aspects are: The effect of variations and uncertainty in heat transfer predictions with cold combustion chamber walls; The impact of the use of ceramic materials on selected engine components over a range of combustion chamber wall temperatures at engine compression ratios of 8 and 16:1.

SIMULATION ASSUMPTIONS

The following assumptions were made in developing the cycle simulation for a conventional spark-ignition engine. Further details can be found in reference (2).

1) The engine cylinder is treated as a variable volume plenum. The cylinder pressure is a function of time only.

2) The charge is homogeneous during intake and compression. During compression, three zones exist within the cylinder: an unburned zone, an adiabatic burned zone, and a boundary layer burned zone. Each zone is uniform in composition and temperature. A schematic of this three zone combustion model is shown in Fig. 1.

3) The volume of gas where the fuel oxidation process occurs is negligible.

4) The individual species in the gas mixture behave as ideal gases. The unburned gas is composed of a non-reacting mixture of air, fuel vapor and residual gases. The fuel in this study was Indolene clear with properties given by LoRusso (3). The burned gases are a mixture of reacting gases, assumed to be in chemical equilibrium. An approximate method for computing burned gas properties is used (4).

5) Quasi-steady, adiabatic and one-dimensional flow equations are used to predict mass flows past the valves. The intake and exhaust manifolds are treated as infinite plenums having specified pressure and temperature histories. When reversed flow past the intake valve occurs, a plug flow model is assumed.

6) Heat transfer is predicted with the correlations of Woschni which were developed for diesel engines and are often applied to spark-ignition engines (5). Additional details of the heat transfer model relevant to the heat transfer studies are given in Appendix A. For each engine component (piston, cylinder wall, cylinder head, valves), the gas-to-wall convective heat transfer is coupled with conduction through the wall and convection to the coolant fluid to obtain the wall temperatures. The coolant temperature and heat transfer coefficients are specified, as are wall thickness and wall thermal conductivity. Thus, the effect of different wall materials, thicknesses, and temperatures can be studied by suitably manipulating this model.

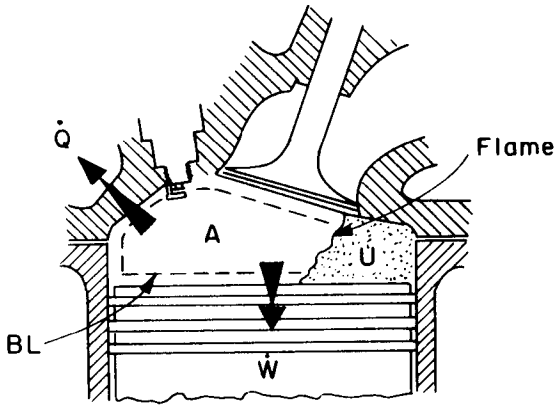

Fig. 1 - Schematic of three zone combustion model. U denotes unburned gas zone; A denotes the adiabatic burned gas core; BL denotes the burned gas boundary layer

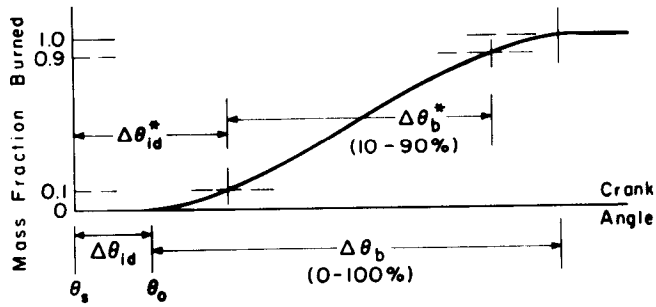

Fig. 2 - Schematic of mass fraction burned profile. Θ_s is the spark timing, Θ_o is the start of combustion, $\Delta\Theta_{id}$ is the ignition delay and $\Delta\Theta_b$ is the combustion duration. $\Delta\Theta_{id}$* and $\Delta\Theta_b$* are the usual empirical definitions of ignition delay and combustion duration (0-10 percent and 10-90 percent burned respectively)

7) The mass fraction burned as a function of crank angle is specified by a Wiebe function of the following form:

$$x = 1 - \exp\{-a[(\Theta - \Theta_o)/\Delta\Theta_b]\}^{m+1} \qquad (1)$$

where:

- x = fraction of total mass in cylinder burned
- a = efficiency parameter
- m = form factor
- Θ = crank angle
- Θ_o = start of combustion
- $\Delta\Theta_b$ = combustion duration

This formulation allows one flexibility in specifying the shape of the curve; the values in this study were determined by matching with experimental traces and were a = 5, m = 2.2 (2).

Figure 2 shows the parameters which define the start and duration of the combustion process. Θ_o, the crank angle at start of combustion, must be specified as input. Θ_o is related to actual spark timing by an ignition delay, $\Delta\Theta_{id}$, as shown. (This ignition delay differs from an empirical ignition delay often used, $\Delta\Theta^*_{id}$, which is the crank angle interval between spark and 10 percent mass fraction burned.) Θ_o is usually related to start-of-combustion-timing which gives maximum-brake-torque at constant inlet pressure (MBT timing). The combustion duration $\Delta\Theta_b$, is also specified as an input. This is the crank angle interval from start of combustion to the 100 percent burned position of the curve in Fig. 2. (This combustion duration (0 to 100 percent) differs from the 10 to 90 percent burn duration $\Delta\Theta^*_b$ often used empirically.)

8) Nitric oxide emissions are calculated by using the extended Zeldovich kinetic scheme, with the steady-state assumption made for the N concentration and equilibrium values used for H, O, O_2 and OH concentrations in the adiabatic core burned gases. A sudden freezing assumption is used for calculating boundary layer NO, which assumes that the NO accompanying the mass transfer into the boundary layer is immediately frozen.

Most of the above assumptions have been used previously in cycle simulations and have been shown valid under normal engine operating conditions.

VALIDATION OF WOT PREDICTIONS

Experimental validation of this cycle simulation for part-throttle engine operation has already been presented by Heywood, et al. (2) A valuable use of engine simulations is in the determination of the dimensions, etc., of a new engine concept which would meet a given wide-open-throttle (WOT) torque-speed requirement. Validation of simulation predictions of WOT performance is therefore important. An example of the simulation output at WOT for a 5.7ℓ naturally aspirated engine is shown in Fig. 3. Cylinder volume, valve lift profiles, inlet and exhaust mass flow rates, cylinder pressure, mass fraction burned, unburned and burned gas temperatures, nitric oxide concentration, heat transfer rate and thermal boundary layer thickness are shown, as function of crank angle, through the four-stroke engine cycle. This operating condition is close to the maximum torque point. The geometric details for this engine are given in Table 1. The operating conditions and the power, mean effective pressure, specific fuel consumption and specific nitric oxide emissions are given in Table 2. To obtain the brake values of engine parameters, mechanical friction was calculated using the method proposed by Bishop (6). Since the simulation covers the complete four-stroke cycle, pumping work over the intake and exhaust strokes is already

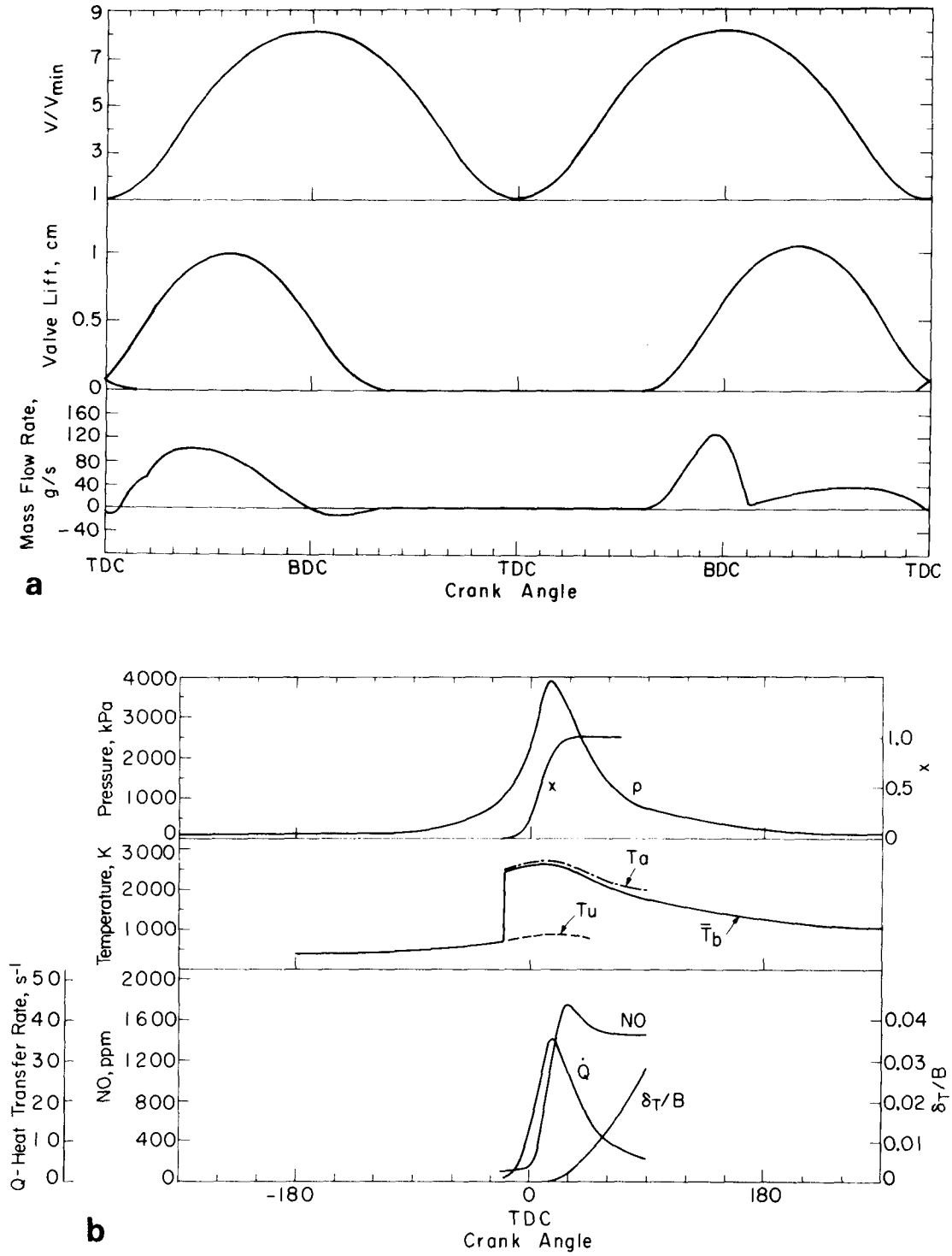

Fig. 3 - Profiles of variables predicted by the simulation throughout the four-stroke engine cycle for a 5.7ℓ engine at WOT and 2500 rev/min. Plotted against crank angle are: cylinder volume/clearance volume, inlet and exhaust valve lift, inlet and exhaust mass flow rates, cylinder pressure p, mass fraction burned x, unburned mixture temperature T_u, mean burned gas temperature $\bar{T}_b$, temperature of burned gas adiabatic core T_a, instantaneous heat transfer rate $\dot{Q}$ (normalized by the initial enthalpy of the fuel-air mixture within the cylinder), nitric oxide concentration NO, thermal boundary layer thickness δ_T (normalized by the cylinder bore B). Details in Table 2

Table 1 - Engine Specifications

	Engine		
	5.7ℓ N.A.	3.8ℓ N.A.	3.8ℓ Turbo
Number of cylinders	8	6	6
Bore (mm)	101.6	96.5	96.5
Stroke (mm)	88.4	86.4	86.4
Crank radius/con. rod length	0.305	0.285	0.285
Compression ratio	8.1:1	8.0:1	8.0:1
Cylinder head area (excl. valves) /piston area	0.91	0.91	0.91
Intake Valve:			
diameter (mm)	50.8	41.3	41.3
max. valve lift (mm)	9.75	9.88	8.15
opens at	38° BTC	41° BTC	41° BTC
closes at	92° ABC	101° ABC	81° ABC
Exhaust valve:			
diameter (mm)	39.6	36.2	36.2
max. valve lift (mm)	10.3	9.45	9.45
opens at	92° ATC	85° ATC	85° ATC
closes at	52° ATC	61° ATC	61° ATC

Table 2 - Simulation Data for 5.7ℓ WOT (Maximum Torque Case)

1. Input		
equivalence ratio, ϕ		1.1
exhaust gas recycle, percent		0
start of combustion timing (MBT), Θ_o		20° BTC
combustion duration, $\Delta\Theta_b$		50°
speed, N rev/min		2500
fuel heating value		43.0 MJ/kg
stoichiometric air-fuel ratio		14.7
fuel molecular composition		$C_{7.26}H_{13.87}$
inlet manifold pressure, kPa		95.1
inlet mixture temperature, K		319

2. Cycle Output	Indicated		Brake
	Gross*	Net*	
power, kW	109.7	104.6	93.0
mean effective pressure, kPa	918.4	875.7	778.4
specific fuel consumption, g/kW-hr	253.7	265.8	299.3
thermal efficiency, %	33.0	31.5	28.0
heat transfer, %	16.9	16.9	16.9
specific NO emissions, gNO/kW-hr	6.07	6.36	7.16

*Gross: Integrated over compression and expansion strokes.
Net: Integrated over full four-stroke cycle.

Table 3 - 5.7ℓ WOT Performance Simulation Test Matrix

Study	Speed rev/min	ϕ	Θ_o °BTC	$\Delta\Theta_b$ °	P_{in} psig	P_{ex} psig	T_{in} °F
1, 3	1000	1.10	10	37	-.12	0.78	115
	2500	1.10	20	50	-.41	4.99	115
	3000	1.10	23	53	-.49	7.54	115
	4000	1.10	25	58	-.67	11.31	115
	4400	1.10	26	60	-.73	11.95	115
2	1000	1.14	10	37	-.12	0.78	115
	2000	1.10	17	46	-.32	3.13	115
	2500	1.13	20	50	-.41	4.99	115
	3000	1.16	23	53	-.49	7.54	115
	4000	1.26	25	58	-.67	11.31	115
	4400	1.26	26	60	-.73	11.95	115

Table 4 - 3.8ℓ Turbocharged Maximum Performance Simulation Test Matrix

Study	Speed rev/min	ϕ	Θ_o °BTC	$\Delta\Theta_b$ °	P_{in} psig	P_{ex} psig	T_{in} °F
1	1200	1.2	10	37	0.98	2.4	98
	1500	1.2	13	40	1.96	3.5	103
	2000	1.2	15	44	5.53	6.9	122
	2500	1.2	18	48	9.50	12.2	159
	3000	1.2	21	50	9.89	15.2	169
	3500	1.2	24	53	9.99	17.3	178
	4000	1.2	26	55	9.94	18.6	190
	4400	1.2	27	57	9.89	19.0	200
2	3000	1.2	10	50	9.89	15.2	169
	3500	1.2	13	53	9.99	17.3	178
	4000	1.2	18	55	9.94	18.6	190
	4400	1.2	19	57	9.89	19.0	200
3	3000	1.2	10	66	9.89	15.2	169
	3500	1.2	13	69	9.99	17.3	178
	4000	1.2	18	71	9.94	18.6	190
	4400	1.2	19	73	9.89	19.0	200
4,5	1200	1.15	10	40	0.98	2.4	98
	1500	1.15	13	43	1.96	3.5	103
	2000	1.15	15	47	5.53	6.9	122
	2500	1.15	10	65	9.50	12.2	159
	3000	1.15	10	70	9.89	15.2	169
	3500	1.15	13	73	9.99	17.3	178
	4000	1.25	18	76	9.94	18.6	190
	4400	1.25	19	79	9.89	19.0	200

determined. (Alternatively, the actual values of friction power (or friction mean effective pressure), taken from manufacturer's data (GM Test Code #11 (7)), were used to obtain brake values.)

Calculations were carried out for the 5.7ℓ naturally-aspirated engine and the 3.8ℓ turbocharged engine listed in Table 1, at wide-open-throttle, over the speed range 1000 to 4400 rev/min. The simulation output was checked against WOT performance data provided by Chevrolet and Buick (GM Test Code #1 (7)). The data provided were inlet manifold pressure, exhaust manifold pressure, spark timing, brake power, brake specific fuel consumption, and friction power as a function of engine speed. Details of this data can be found in references (8) and (9). Wallace (8) provides a description of the two engine systems examined in this study.

Although most of the simulation input parameters required for calculations which predict these engines WOT performance were provided by the manufacturer's data, it was necessary to determine ignition delay, ($\Delta\Theta_{id}$), to relate the crank angle for start-of-combustion in the simulation (Θ_o) to the actual engine spark timing (Θ_s), and to determine a combustion duration ($\Delta\Theta_b$), for the given operating condition. (Figure 2 shows the relationship between these variables.) An outline of the procedure used to determine $\Delta\Theta_{id}$ and $\Delta\Theta_b$ is given in Appendix B. Correlations developed by Hires, et al. (10) for ignition delay and burn duration as functions of engine speed, critical engine dimensions and laminar flame speed were used. Both ignition delay and burn duration increase simultaneously over the speed range 1000 to 4400 rev/min.

Also, it was necessary to estimate the fuel-air equivalence ratio (ϕ) metered by the carburetor at each load and speed point. Where allowance for varying ϕ with load and speed was made, manufacturer's carburetor flow data was used for this purpose.

The inlet mixture temperature was also estimated. For turbocharged engine operation data provided by AirResearch was used for this purpose.

Tables 3 and 4 give the input parameters: equivalence ratio ϕ, start of combustion Θ_o, burn duration $\Delta\Theta_b$, inlet and exhaust manifold pressures P_{in} and P_{ex}, and inlet mixture temperature for the WOT studies.

Figures 4 and 5 show the comparison between the brake mean effective pressures (bmep) and brake specific fuel consumption

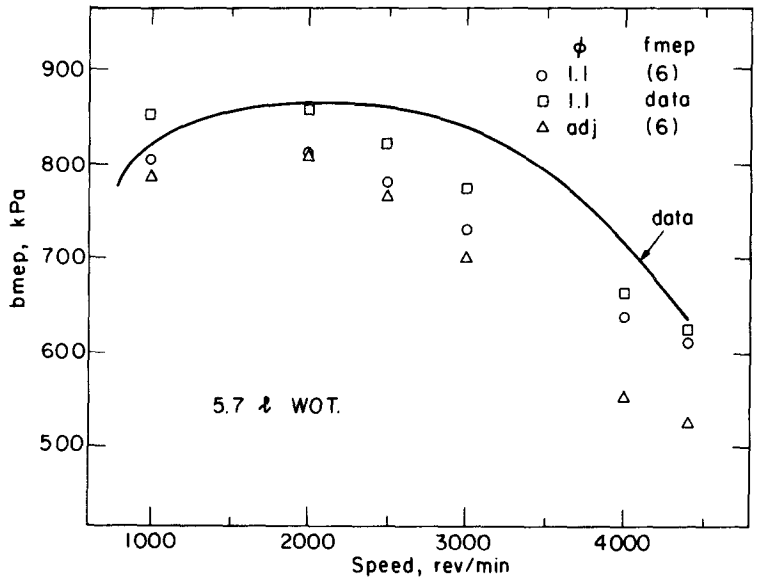

Fig. 4 - Comparison of bmep predicted by the simulation with engine test data at varying speeds for a 5.7ℓ engine at WOT. See Table 3

(bsfc) of the actual engine and the simulation output at WOT for the naturally aspirated 5.7ℓ engine. A series of calculations were done to explore the effect of several factors on the quality of the match: 1) equivalence ratio held constant at $\phi = 1.1$; 2) equivalence ratio varied to account for the changing air-fuel ratio with engine speed; and 3) equivalence ratio held constant and bmep values obtained using actual fmep data instead of fmep based on Bishop's model (6).

Figure 4 shows that the simulation adequately predicts bmep over the lower half of the speed range, but underpredicts bmep by about 10 to 15 percent at the higher engine speeds. Figure 5 shows reasonable agreement in bsfc at the highest engine speeds, but the simulation underpredicts bsfc by 15 to 20 percent in the low and mid speed range.

Figures 6 and 7 show bmep and bsfc comparisons of the simulation output with WOT data for the turbocharged 3.8ℓ engine. Again, to examine the influence of various factors on the quality of the match, several sets of calculations were carried out: 1) MBT timing with ϕ held constant at 1.2; 2) retarded timing at speeds of 2500 rev/min and greater, to match the engines' spark advance curve, with $\phi = 1.2$; 3) retarded timing, $\phi = 1.2$, and $\Delta\theta_b$ adjusted to allow for the retarded timing; 4) retarded timing, ϕ adjusted to account for the changing metering characteristics of the carburetor with airflow, and $\Delta\theta_b$ adjusted to allow for retarded timing and variation in equivalence ratio; 5) similar to study 4 except that actual fmep data were used to compute bmep.

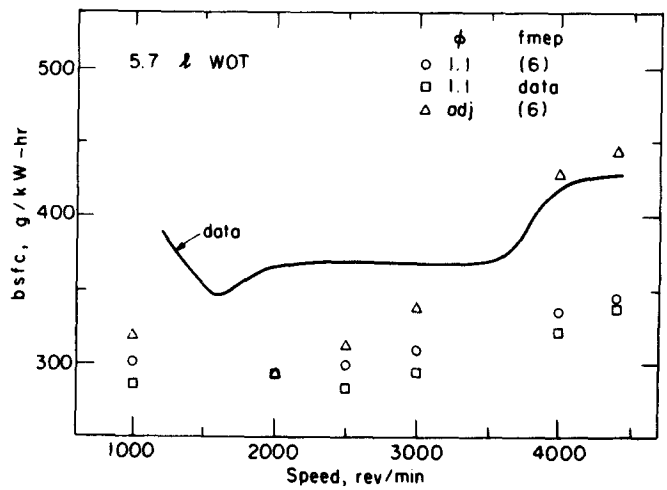

Fig. 5 - Comparison of bsfc values predicted by the simulation with engine test data at varying speeds for a 5.7ℓ engine at WOT. See Table 3

Figure 6 shows close agreement between the bmep values from the simulation output and the engine data using MBT timing up to approximately 2500 rev/min. At this point, knock would occur in the engine due to the high inlet pressures, so the spark timing is retarded approximately 8 degrees at 2500 rev/min and then advanced from this point for higher speeds (8). As a result, the simulation output with MBT timing diverges from the data at speeds of 2500 rev/min and greater. The subsequent studies, in which spark timing, burn duration and equivalence ratio were

adjusted to represent better the actual engine operating characteristics, improved the match with the test data to within a modest margin of error.

Figure 7 shows the comparison of the bsfc values predicted by the simulation with the turbocharged engine bsfc data. The predicted bsfc values fall about 15 percent below the actual data up to about 3000 rev/min. Agreement above 3500 rev/min is better, less than 10 percent below the data. The trends shown by study 5) (the dashed line), which should give the best match to the engine data, closely match the experimental trends.

In evaluating these results it is useful to distinguish two sources of uncertainty: 1) uncertainties in matching the simulation to the engine test conditions and 2) inadequacies or omissions in the model itself.

The primary uncertainties in matching the engine test conditions are in the equivalence ratio metered by the carburetor, and the value of the fmep. Equivalence ratios were estimated using steady-flow carburetor test-stand data. At wide-open-throttle, the pulsations in carburetor-venturi air-flow, due to the filling of each cylinder in turn, increase the effective fuel metering signal relative to the signal for a steady flow at the same average flow rate. An enhancement of the fuel metering signal at WOT by about 20 percent is plausible, based on an empirical equation derived by Harrington and Bolt (11). This enhancement is inversely proportional to engine speed; thus, it is greatest at the lowest engine speeds, and decreases as speed increases. We judge this the most important contribution to the discrepancy between bsfc predictions and experimental data in the naturally aspirated engine comparison. In the turbocharged engine case, the carburetor is upstream of the turbocharger so this enhancement would be much reduced. However, the carburetor calibration in the mid and high speed range may have been richened to delay the onset of knock. The uncertainty in fmep is due to the fact that fmep is measured under motoring and not firing conditions (7) but is likely to have a smaller effect than equivalence ratio uncertainties.

If bsfc predictions were increased by 10 to 20 percent for the above reasons to match the data, then bmep predictions would be higher than the experimental bmep data. The following factors which are not included in the simulation would explain bmep predictions higher than the data: 1) Cylinder-to-cylinder nonuniformities in equivalence ratio; in the simulation, all the cylinders are assumed to contain a uniform fuel-air mixture at the same equivalence ratio; 2) omission of crankcase blow-by; 3) omission of flame quenching and hydrocarbon emissions formation phenomena; only about 95 percent of the fuel fed to the

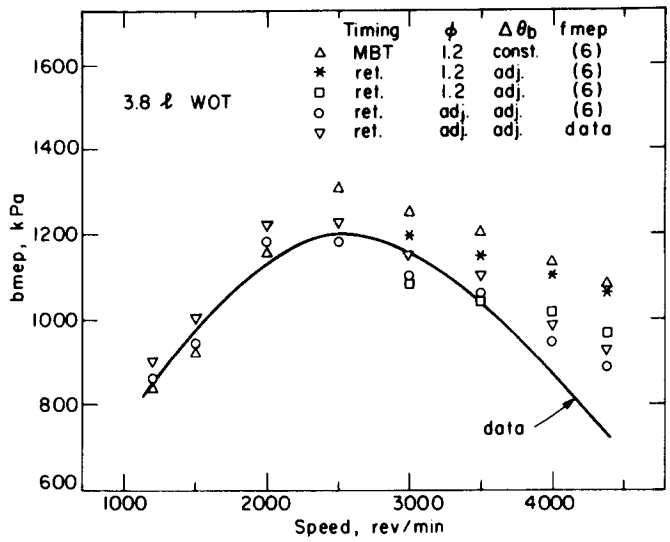

Fig. 6 - Comparison of bmep values predicted by the simulation with engine test data at varying speeds for a 3.8ℓ turbocharged engine at maximum output power. See Table 4

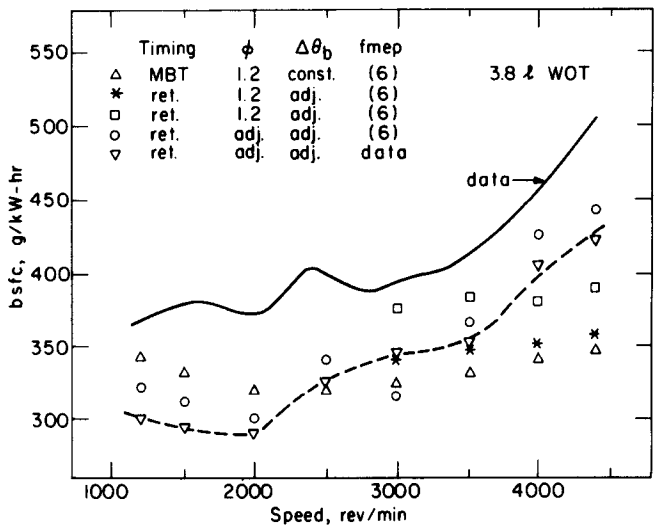

Fig. 7 - Comparison of bsfc values predicted by the simulation with engine test data at varying speeds for a 3.8ℓ turbocharged engine at maximum output power. See Table 4

engine burns in the cylinder. All these factors would decrease bmep for a given bsfc.

There are additional uncertainties in matching the inlet mixture temperature, the ignition delay and the combustion duration of the simulation to the experiment. There could also be errors introduced by the heat transfer correlation and the use of quasi-steady one-dimensional flow equations to predict the inlet and exhaust flows. While the contribution from each of these considerations separately is likely to be small, the

net effect may be more significant. However, it is the trend prediction capability of the simulation which is most important, and Figs. 4 to 7 indicate this is satisfactory.

VALIDATION OF TURBOCHARGED ENGINE OPERATION AT PART LOAD

An additional model validation study was performed to examine the ability of the simulation to predict the turbocharged engine's performance over the complete load range at a constant speed. This was necessary to determine if accurate predictions of the turbocharged engine's performance could be made by calculating the engine's exhaust pressure and inlet temperature from compressor and turbine maps rather than using measured engine test data. An engine speed of 2000 rev/min was selected for this study; the turbocharger affects engine performance over about half of the engine load range.

The combustion parameters for the simulation were determined as described in Appendix B. The start-of-combustion timing Θ_o, was related to manufacturer's spark timing data through the ignition delay $\Delta\Theta_{id}$. The burn duration $\Delta\Theta_b$, and $\Delta\Theta_{id}$, were determined from the correlations of Hires et al. (10). The equivalence ratio assumed ranged from stoichiometric to fuel-rich to match with high load operating conditions. The intake pressures were taken from manufacturer's data. Details of the input parameters are given in Table 5.

Figure 8 shows the comparison of the bmep values predicted by the simulation and the 3.8ℓ turbocharged engine data. A series of simulation studies were made: 1) Using motored engine fmep data to obtain brake values from calculated indicated values; 2) Using Bishop's formulas (6) to determine fmep and, thus, brake values; 3) Using Bishop's formulas for fmep and adding an estimate of the power requirements of the engine's auxilliaries such as the generator, air pump, water and oil pumps, and fan (12). Figure 9 shows the comparison of bsfc values predicted by the engine simulation and the engine data.

At the high end of the load range, bmep is overpredicted which results in an underprediction of bsfc. The previous comments about cylinder-to-cylinder nonuniformities in equivalence ratio and the omission of blowby and quenching apply here, and are the probable cause of this discrepancy. In the low load range, the assumed equivalence ratio of 1.0 may be too lean, and these same factors will also apply. The inclusion of accessory power requirements improves the match significantly at the low load end of the range. Given the uncertainties in some of the engine operating conditions and in the matching process, and the omissions from the model, the agreement was judged adequate for the simulation to be a useful predictor of engine performance.

Table 5 - 3.8ℓ Turbocharged Part Load Simulation Test Matrix

Speed rev/min	$\Delta\Theta_b$ °	Θ_o °BTC	ϕ	P_{in} psig	P_{ex} psig	T_{in} °F
2000	94	32	1.00	-6.76	0.50	96
2000	63	26	1.10	-3.67	0.50	98
2000	63	26	1.10	-0.49	2.96	98
2000	47	18	1.10	1.76	5.25	105
2000	47	15	1.15	3.72	5.94	118

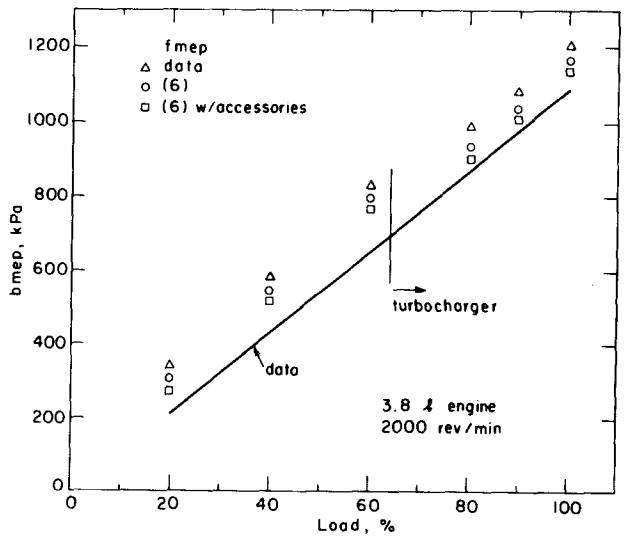

Fig. 8 - Comparison of bmep values predicted by the simulation with engine test data at varying loads for the 3.8ℓ turbocharged engine at 2000 rev/min. See Table 5

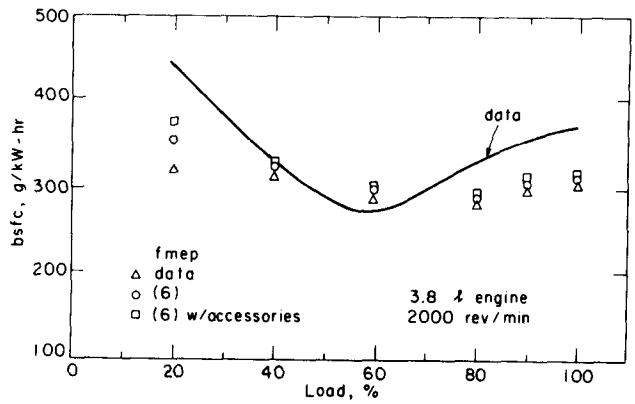

Fig. 9 - Comparison of bsfc values predicted by the simulation with engine test data at varying loads for the 3.8ℓ turbocharged engine at 2000 rev/min. See Table 5

COMPARISON OF NATURALLY-ASPIRATED AND TURBOCHARGED ENGINE OPERATION

The fundamentals of turbocharging spark-ignition engines for increased power have been summarized recently by Wallace (8). By increasing the density of the fuel-air mixture

delivered to the engine at high engine loads, the maximum power of a given displacement engine is increased. Thus a turbocharged engine can provide the same maximum power as a larger displacement naturally-aspirated engine. At part-throttle conditions where the turbocharger has a negligible effect on engine operation, the turbocharged engine will have a higher efficiency than the naturally-aspirated engine, because its displacement is lower, and at the same brake load its inlet pressure and hence mechanical efficiency are higher.

A simulation of the type described here can be used to size a turbocharged engine so that it provides equal maximum torque to a naturally-aspirated engine of given displacement (or check that a given turbocharged engine provides equal maximum torque). It can then be used to compare the two engines over any part of the brake-load/speed map of interest in a particular vehicle application. With the simulation, everything other than the geometry of these two engines and the fact that one is turbocharged, can be made the same. The effect of turbocharging alone, therefore, can be defined. In contrast, the operating conditions of the production 3.8ℓ turbocharged and 5.7ℓ naturally-aspirated engines studied in the previous section are not identical (see Tables 3 and 4).

A comparative study of the 3.8ℓ turbocharged and 5.7ℓ naturally-aspirated engines, whose geometries are described in Table 1, was carried out with identical operating conditions (other than those related to the turbocharger) for each engine. Table 6 summarizes the main input parameters. Stoichiometric operation with MBT timing and constant burn duration of 60° was assumed. For the 3.8ℓ turbocharged engine, the input parameters inlet pressure and inlet mixture temperature were assumed the same as manufacturer's data for the production engine. The turbocharger turbine and compressor maps were used to obtain the exhaust pressure level consistant with the mass flow rate and turbocharger speed.

Figure 10 shows the comparison of bsfc for the 3.8ℓ turbocharged engine and the 5.7ℓ naturally aspirated engine as a function of engine brake power at selected engine speeds. At the speed for the maximum torque (3200 rev/min) the two engines provide the same brake power, as expected. At any given power level the 3.8ℓ turbocharged engine exhibits lower fuel consumption than the 5.7ℓ engine. At a moderate vehicle acceleration point (e.g., brake power ≈ 40 kW and an engine speed of 2000 rev/min), the reduction in fuel consumption for the smaller displacement engine is approximately 9 percent. At this point, the turbocharger is actually "idling" and rotating at relatively slow speeds; the turbocharged engine is performing essentially as a naturally-aspirated engine and the improvement in bsfc comes from the improved mechanical efficiency of the engine. As the demand for power is increased the turbocharger comes into effect and positive manifold pressures are realized. However, at low engine speeds such as 1200 rev/min, the turbocharger has very little effect and the maximum power the 3.8ℓ engine can develop for the conditions of this study is approximately 3 percent less than the 5.7ℓ engine.

A fuel economy gain for the 3.8ℓ engine is shown in Fig. 10 for each brake power level. In practice at wide-open-throttle, for both engines the incoming charge will be richened, to increase power. The turbocharged engine may require an even richer mixture and retarded timing to avoid knock. A comparison of the actual engine data at maximum power

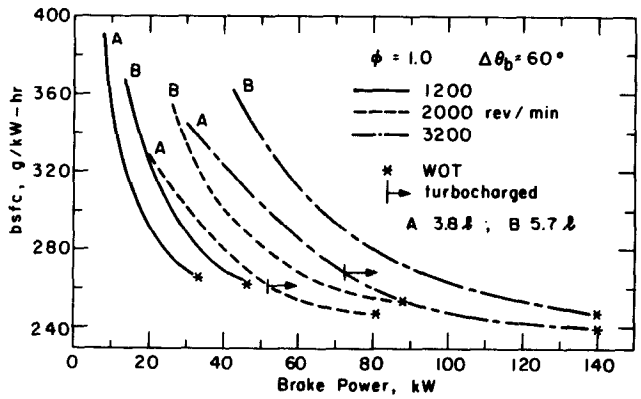

Fig. 10 - Comparison of the bsfc versus power output of the 3.8ℓ turbocharged and 5.7ℓ naturally aspirated engines at three speeds. MBT timing; see Table 6

Table 6 - Data for Comparison of the 3.8ℓ Turbocharged and 5.7ℓ Engines

Engine	Speed rev/min	ϕ	θ_o °BTC	$\Delta\theta_b$ °	P_{in} psig	P_{ex} psig	T_{in} °F
3.8ℓ	1200	1.0	21	60	-7.74 to 0.59	0.5 to 2.0	98 to 112
3.8ℓ	2000	1.0	23	60	-6.76 to 5.53	0.5 to 6.9	98 to 122
3.8ℓ	3200	1.0	25	60	-7.03 to 9.99	0.5 to 16.2	98 to 174
5.7ℓ	1200	1.0	21	60	-7.74 to WOT	0.5	98
5.7ℓ	2000	1.0	23	60	-7.74 to WOT	0.5	98
5.7ℓ	3200	1.0	25	60	-7.74 to WOT	0.5	98